ARTICLES

Trends in Vibrational Frequencies of Guests Trapped in Clathrate Hydrate Cages

Sivakumar Subramanian[†] and E. Dendy Sloan, Jr.*

Center for Hydrate Research, Department of Chemical Engineering, Colorado School of Mines, Golden, Colorado 80401

Received: September 27, 2001; In Final Form: January 7, 2002

Raman spectra of ethane trapped in the small 5^{12} cage of sII hydrate (at ∼70 MPa), isobutane trapped in the large $5^{12}6^4$ cage of sII hydrate, and the gauche form of *n*-butane trapped in the large $5^{12}6^4$ cage of sII hydrate were obtained for the first time. These new Raman results are combined with existing Raman and IR results for various guests to infer general trends in vibrational frequencies of guest molecules trapped in clathrate hydrate cages as a function of cage size, guest size, guest vibrational mode, and pressure. The observed trend in stretching frequencies of guests with cage size, which can be stated as "the larger the cavity, the lower the frequency", is explained through the qualitative "loose cage−tight cage" model of Pimentel and Charles (*Pure Appl. Chem.* **1963**, 7, 111).

Introduction

Clathrate hydrates are crystalline inclusion compounds that consist of guest molecules of suitable sizes and shapes trapped in well-defined cavities formed by water molecules. There are three known crystal structures for hydrates of hydrocarbons: sI, sII, and sH. Properties of these crystal structures and information on the molecules that serve as guests in these structures can be found in the literature.[1−4]

Vibrational spectra (Raman and IR) of guests have provided vital information on clathrate hydrates for the past few decades. Molecular vibrations of both the guest and host molecules in the hydrate lattice have been probed using Raman spectroscopy. Information regarding structure of the hydrate, formation/dissociation mechanisms, cage occupancies, hydrate composition, and molecular dynamics has been obtained.[5−12] In such studies, it is important to establish which bands in the Raman spectrum of the guest molecule correspond to which hydrate cage.

In this paper, the issue of perturbation of the vibrational energy levels of a guest molecule trapped in a cage by the water molecules forming the cage will be addressed. New Raman results for guests ethane, isobutane, and *n*-butane in sII hydrate will be presented in the first part of the paper. These will be combined in the latter part of the paper with existing IR and Raman results for various guests in different hydrate cages to elucidate general trends in guest molecule vibrational frequencies as a function of cage size, guest size, guest vibrational mode, and pressure. The observed trends in vibrational frequencies will be explained using the qualitative "loose cage−tight cage" model of Pimentel and Charles.[13]

* Corresponding author. Telephone: 303-273-3723. Fax: 303-273-3730. E-mail: esloan@mines.edu.

[†] Currently at ChevronTexaco EPTC, 2811 Hayes Road, Houston, TX 77082.

Experimental Details

New Raman Results For Ethane, Isobutane, and n-Butane in sII Hydrate. The multichannel Raman spectrometer used in this work has been described in detail elsewhere.[10,11] Raman spectra of ethane, isobutane, and *n*-butane in sII hydrate were recorded by integrating the backscattered signal between 500 and 5000 s depending on the quality of the signal. GRAMS/32 was used to analyze the data.

Raman spectra pertaining to ethane in sII hydrate were obtained at high pressures (∼70 MPa) using a brass cell fitted with sapphire windows. Details about the cell and the experimental setup can be found elsewhere.[14] Spectra corresponding to isobutane and *n*-butane in sII hydrates were obtained at pressures less than 2 MPa using the thick-walled Pyrex capillary cell setup, details of which can also been found elsewhere.[6]

Results and Discussion

Raman Spectrum of Ethane in sII Hydrate at High Pressure. Hydrate prediction models generated over the last several decades have assumed that ethane only enters the $5^{12}6^2$ and $5^{12}6^4$ cavities in sI and sII, respectively. However, a recent Raman study of pure ethane sI hydrate in the pressure range of 20−479 MPa concluded that ethane occupies the small 5^{12} cages in the lattice at these pressures.[15] This conclusion was reached based upon splitting of the ν_3 symmetric C−C stretching band into two distinct peaks. The intense peak centered around 1000 cm^{-1} over the entire pressure range was assigned to C_2H_6 in the $5^{12}6^2$ cage.[15] The comparatively weaker second peak, which increased in frequency (and intensity) from 1019 cm^{-1} at 20 MPa to ∼1023 cm^{-1} at 479 MPa, was assigned to C_2H_6 in the small 5^{12} hydrate cage.[15] The observed increase in intensity of this peak with pressure was attributed to an increase in occupation of the 5^{12} cavity by ethane.[15]

In the present work, Raman spectrum of a sII hydrate of ethane and tetrahydrofuran (THF) was obtained at 70.7 MPa to

10.1021/jp013644h CCC: $22.00
Published on Web 04/06/2002

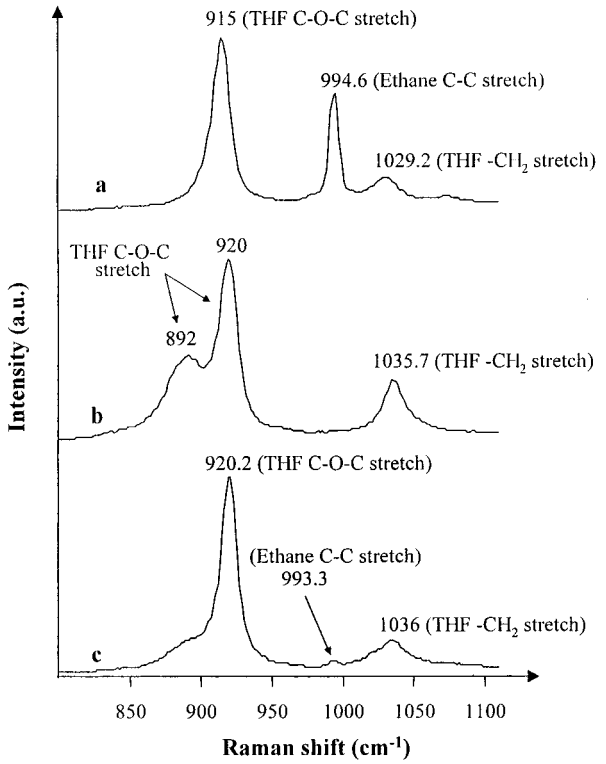

Figure 1. Raman spectra showing the C−C stretching vibration of ethane and the C−O−C stretching and CH_2 vibrations of THF in (a) organic liquid phase, (b) aqueous phase, and (c) hydrate phase, at 70.7 MPa and 277.2 K.

investigate the possible occupation of the sII 5^{12} cage by ethane at high pressures. THF was chosen as the other guest because it is well-established that this water-miscible guest forms sII hydrate by itself.[16]

To form the hydrate sample in the high-pressure optical cell, 0.3 cm^3 of spectroscopic-grade liquid THF (from Fischer Scientific) was loaded into the cell followed by charging with ethane gas (99.5% purity) to ∼4 MPa. Pumping liquid water into the cell caused ethane vapor to condense, thus yielding two immiscible liquid phases: an ethane-rich liquid hydrocarbon phase and an aqueous phase. THF partitioned between the two phases. Further pumping of liquid water caused cell pressure to rapidly increase to the final value of 70.7 MPa. The molar ratio of ethane to THF in the final sample was estimated to be 1.3. The cell was then mounted on a precision *XY* stage, and Raman spectra corresponding to the two liquid phases were recorded by focusing the laser on each phase. Hydrate crystal formation at the liquid−liquid interface was induced by cooling the cell from 298.2 to 277.2 K at a rate of 0.62 K per min. The cell was conditioned at 277.2 K and 70.7 MPa for several hours. Raman spectra of the hydrate phase were then recorded by focusing the laser on hydrate needles at the interface.

Figure 1 shows a stacked plot of three Raman spectra, marked a−c, over the frequency range of 800−1120 cm^{-1}. Spectrum a corresponds to the organic liquid phase (liquid ethane + THF + small amount of water); spectrum b corresponds to the aqueous phase (water + THF + small amount of ethane); and spectrum c corresponds to the hydrate phase. In all three spectra, the most intense band occurs in the 915−920 cm^{-1} region. This band corresponds to the C−O−C stretching vibration of THF in each of the phases. The 990−1000 cm^{-1} region in each spectrum corresponds to the ν_3 C−C stretching vibration of ethane in each of the phases. The 1029−1036 cm^{-1} region in each spectrum corresponds to a CH_2 stretching vibration of THF.

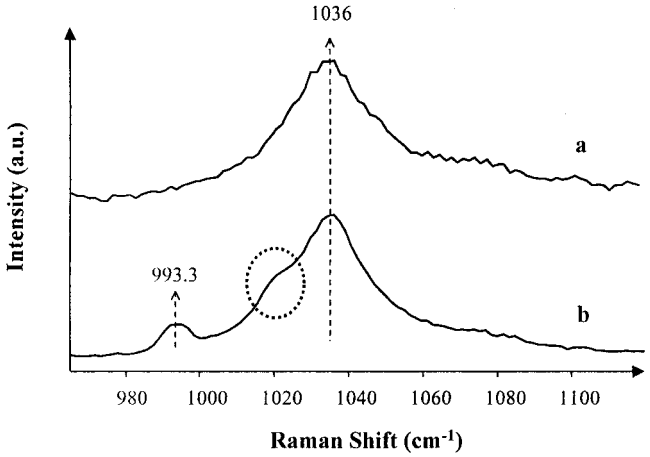

Figure 2. Comparison of Raman spectra of (a) pure THF sII hydrate (0.1 MPa and 277.2 K) and (b) C_2H_6 + THF sII hydrate (70.7 MPa and 277.2 K). Spectrum b is a magnified version of spectrum c in Figure 1.

Prominent bands are observed in all three regions (915−920, 990−1000, and 1029−1036 cm^{-1}) in spectrum a, suggesting that the organic liquid phase contains significant amounts of both THF and ethane. In spectrum b, the bands due to THF are intense (915−920 and 1029−1036 cm^{-1} regions), whereas no prominent peak is observed for ethane (990−1000 cm^{-1}). This suggests that there is little ethane in the aqueous phase which agrees well with the very low solubility of ethane in water (<0.1 mol % at these conditions in the absence of THF).[17] The broad low frequency shoulder at 892 cm^{-1} on the 920 cm^{-1} C−O−C stretching band of THF can be attributed to the C−O−C stretching vibration of THF that is hydrogen-bonded to the surrounding water molecules.[18] It should be noted that no such shoulder is observed on the 1035.7 cm^{-1} band of THF.

In spectrum c for the hydrate phase, THF bands at 920.2 and 1036 cm^{-1} are prominent. The absence of a prominent shoulder around 892 cm^{-1} on the 920.2 cm^{-1} THF C−O−C stretching band can be attributed to breaking of the hydrogen bonds between THF and water, and this is strong evidence for enclathration of THF in the $5^{12}6^4$ cage of sII hydrate.[18] A weak peak in the 990−1000 cm^{-1} range, corresponding to the ν_3 symmetric C−C stretching vibration of ethane, can also be detected in spectrum c. The frequency of this band is 993.3 cm^{-1}, which compares well with the 992.9 cm^{-1} value for ethane in the $5^{12}6^4$ cavity of sII at ∼1 MPa,[11] suggesting that the hydrate responsible for spectrum c is of type sII.

To explore whether ethane enters the small 5^{12} cavity of sII hydrate, a magnified version of spectrum c in Figure 1 is shown as spectrum b in Figure 2. Spectrum a in Figure 2 is that of pure THF sII hydrate at atmospheric pressure and 277.2 K, formed in a Pyrex capillary cell from a solution with a THF/water molar ratio of 1:15.3. The 965−1120 cm^{-1} spectral window in Figure 2 was chosen to concentrate on the C−C stretching region of C_2H_6 and the CH_2 stretching mode of THF (1029−1036 cm^{-1} region).

The intense feature in spectra a and b in Figure 2 is the band at 1036 cm^{-1} due to the CH_2 stretching vibration of THF in the $5^{12}6^4$ cage of sII. This band is symmetric in shape in spectrum a and does not have any shoulders. In spectrum b, the 993.3 cm^{-1} band for C−C stretching of ethane in the $5^{12}6^4$ cavity of sII is readily visible in addition to the 1036 cm^{-1} band of THF. It can also be clearly seen from spectrum b that there is a distinct low frequency shoulder at about 1020 cm^{-1} on the intense 1036 cm^{-1} THF band. This shoulder, highlighted using a dotted

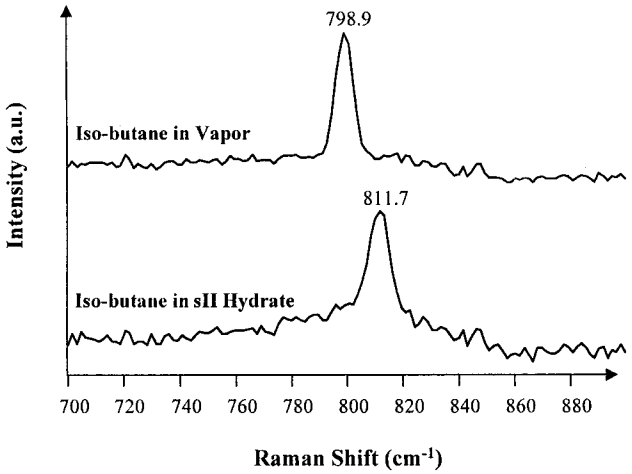

Figure 3. Representative Raman spectra of isobutane vapor (at 0.317 MPa and 295.2 K) and sII isobutane hydrate (at 0.145 MPa and 274.2 K) comparing the symmetric C−C stretching vibration of isobutane in the two phases.

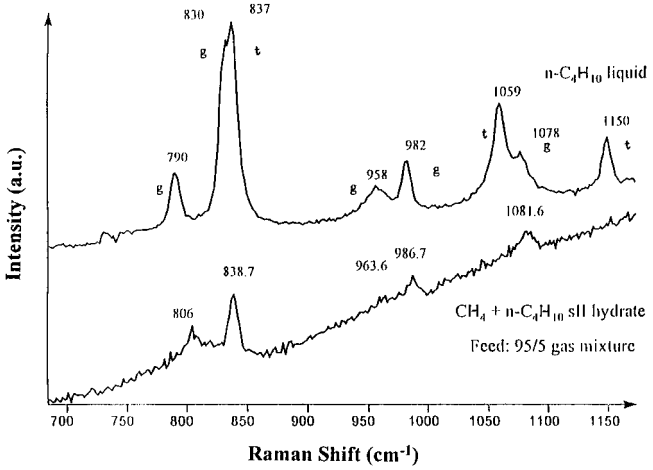

Figure 4. Comparison of the 685−1175 cm^{-1} region in the Raman spectra of pure *n*-butane liquid (at 0.22 MPa and 295.2 K) and methane + *n*-butane sII hydrate (at 1.93 MPa and 273.7 K). The bands marked "t" and "g" in the liquid spectrum correspond to the trans and gauche forms of *n*-butane, respectively.

ellipse, suggests the presence of a new band in spectrum b for THF + ethane sII hydrate. By use of the second derivative of spectrum b, the frequency of the new weak band was determined to be 1019.9 cm^{-1}. This frequency agrees well with that assigned by Morita et al. to the C−C stretching of ethane in the 5^{12} cavity of sI at similar pressures.[15] It should be noted that spectrum b in Figure 2 is only a representative spectrum. Similar analyses of multiple spectra from different spots within the sample confirm the existence of a weak band at ∼1020 cm^{-1}. Consequently, this new weak band at ∼1020 cm^{-1} is assigned to the ν_3 symmetric C−C stretching of ethane trapped in the small 5^{12} cage of sII hydrate.

Raman Spectrum of Isobutane sII Hydrate. Figure 3 compares the Raman spectrum of pure isobutane sII hydrate, formed in the low-pressure capillary optical cell from isobutane gas and DI water at 0.145 MPa and 274.2 K, with the spectrum for isobutane gas at 0.317 MPa and 295.2 K. The $P-T$ condition of the hydrate ensures that there is no liquid isobutane in the sample.

A single intense band is observed in the gas-phase spectrum at 798.9 cm^{-1}, which can be assigned to the ν_7 symmetric C−C stretching vibration of isobutane.[19] The same vibration occurs at 811.7 cm^{-1} when isobutane is trapped in sII hydrate. On the basis of the lack of band splitting and cursory comparison of molecular size of isobutane and sizes of sII hydrate cages,[1,3] the 811.7 cm^{-1} band is assigned to the symmetric C−C stretching of isobutane in the large $5^{12}6^4$ cavity of sII hydrate. The observed 12.8 cm^{-1} (=811.7 − 798.9 cm^{-1}) increase in frequency of this band upon enclathration is similar to the shift observed in the case of the ν_8 C−C stretching mode of propane in the $5^{12}6^4$ cage of sII[6] and the ν_3 C−C stretching mode of ethane in sI hydrate.[11] It should however be noted that an increase of 12.8 cm^{-1}, upon being trapped in the $5^{12}6^4$ cage, is much higher compared to the 7.3 cm^{-1} increase in the case of propane.

Raman Spectrum of Methane + n-Butane sII Hydrate. There are two known rotational isomers of *n*-butane, the trans (chair) and the gauche (boat) forms. It has been well established that distinct contributions from both these forms can be identified in Raman spectra of *n*-butane vapor and liquid.[20−24] It has also been shown that at ∼77 K, the Raman spectrum of solid *n*-butane has contributions only from the lower energy trans form, suggesting that the higher energy gauche form is not stable at that temperature.[20] These studies suggest that Raman spectroscopy can be used to identify the form of *n*-butane present in a sample.

The only molecular measurements in the literature on hydrates containing *n*-butane are the dielectric relaxation studies on a sII hydrate of H_2S + *n*-butane by Davidson et al.[25] The response from only the gauche form of *n*-butane trapped in the hydrate was measured in that study because only the gauche form has a finite permanent dipole moment that is needed to make a molecule detectable in dielectric relaxation studies. On the basis of size considerations, however, Davidson et al. hypothesized that the gauche form (largest van der Waals diameter of 7.1 Å) is probably the only form of *n*-butane that participates in the hydrate lattice and that the trans form is too big in size (largest van der Waals diameter of 7.9 Å) to fit in the $5^{12}6^4$ cage of sII.[25] To date, there is no experimental evidence showing the exclusion of the trans form from the hydrate lattice.

In the present work, the Raman spectrum of *n*-butane liquid at 0.22 MPa and 295.2 K is compared with the spectrum for a sII hydrate of methane + *n*-butane at 1.93 MPa and 273.7 K (Figure 4). The hydrate was formed from a vapor feed of 95 mol % methane and 5 mol % *n*-butane. It was conditioned at the set $P-T$ for several days prior to obtaining the Raman spectrum. The set hydrate $P-T$ condition prevented a liquid hydrocarbon phase from forming and thus ensured that spectral contributions were only from *n*-butane trapped in the hydrate phase.

The poor signal-to-noise (S/N) ratios of the hydrate spectrum (bottom) in Figure 4 and some of the hydrate spectra discussed earlier are attributed to a combination of factors such as low incident laser power, low concentration of hydrates in the scattering volume, and reduced backscattered signal intensity resulting from stray losses because of the curved sample cell + cooling jacket configuration.

In comparison, the liquid *n*-butane spectrum (top) has a better S/N ratio due to a concentrated sample and reduced stray losses. Frequencies of peaks observed in the liquid spectrum are indicated in addition to the labeling of peaks as "t" or "g" corresponding to the trans or the gauche forms of *n*-butane. The assignment of the bands to either the trans or gauche isomers in this spectrum is based on the work of Kint et al.[21] There are two distinct trans−gauche band pairs in this spectrum, at 830(g) − 837(t) cm^{-1} and 1059(t) − 1078(g) cm^{-1}. These band pairs correspond to C−C stretching vibrations of the two forms of

n-butane.[21] Also, the bands at 790, 958 (C−C stretching mode), and 982 cm^{-1} (CH_3 rocking mode) only correspond to the gauche form whereas the 1150 cm^{-1} band (due to CH_3 rocking and C−C stretching modes) is only due to the trans form.[21]

Considering the hydrate phase spectrum, it can be seen that the two trans−gauche band pairs originally present in the liquid spectrum reduce to single bands at 838.7 and 1081.6 cm^{-1}. The 1081.6 cm^{-1} band is slightly higher in frequency compared to the 1078 cm^{-1} band assigned to the gauche form in liquid *n*-butane. The close proximity of these frequencies suggests that the 1081.6 cm^{-1} may be due to the gauche form of *n*-butane trapped in the hydrate. The only other bands in this spectrum are at 806 and 964−987 cm^{-1}. These bands, although shifted to higher frequencies compared to those in the liquid-phase spectrum, can be assigned to the gauche form of *n*-butane in sII hydrate. It can be clearly seen that the bands due to the trans form occurring at 1059 and 1150 cm^{-1} in the liquid spectrum are nonexistent in the hydrate spectrum, implying that the 838.7 cm^{-1} band in the hydrate spectrum must be due to C−C stretching in the gauche form of *n*-butane. Thus, it can be concluded that only bands due to the gauche form of *n*-butane are observed in the sII spectrum in the 685−1175 cm^{-1} range. The trans form is excluded from the hydrate lattice, thus confirming the hypothesis of Davidson et al. that it may be too large to enter the $5^{12}6^4$ cage.[25]

Perturbation of Guest Vibrations upon Enclathration

This section will discuss the perturbation of vibrational energies of a guest molecule trapped in a cage by the water molecules forming the cage using a qualitative loose cage−tight cage model existing in the literature. The model will be used to explain the trends in frequencies observed in Raman and IR spectra of different guests as a function of cage size, guest size, guest vibrational mode, and pressure.

The Loose Cage−Tight Cage Model. The origin of the loose cage−tight cage model lies in the perturbation treatment developed by Buckingham[26] to explain the shifts in the vibrational frequencies of a diatomic solute molecule due to its interaction with a liquid solvent. By treating the interaction and the anharmonic terms in the potential energy function of the free solute molecule as small perturbations to the harmonic potential of the free molecule, the expression in eq 1 for vibrational frequency shift, $\Delta\nu$, was obtained.[26]

$$\Delta\nu = \nu_{\text{solvent}} - \nu_{\text{gas}} = \frac{B_e}{hc\omega_e}\left[U'' - \frac{3A}{\omega_e}U'\right] \qquad (1)$$

In eq 1, ν_{solvent} and ν_{gas} are the vibrational frequencies of the solute in the solvent and in the free gas respectively; B_e is the equilibrium rotational constant in inverse centimeters; ω_e is the "classical" frequency of the harmonic oscillator in inverse centimeters; U' and U'' are, respectively, the first and second derivatives of the solute−solvent interaction potential with respect to the dimensionless displacement coordinate $(r - r_e)/r_e$, averaged over all solvent configurations where r_e is the equilibrium bond length and $(r - r_e)$ is the displacement from the equilibrium position; A is the anharmonicity constant expressed in inverse centimeters; h is Planck's constant; and c is the speed of light.

Pimentel and Charles substituted the expressions for B_e and ω_e in eq 2 into the basic expression for $\Delta\nu$ in eq 1 and extended it to generate eq 3 for the shift in vibrational frequencies of polyatomic molecules trapped in matrixes due to the interactions between the trapped molecules and the molecules forming the matrix.[13]

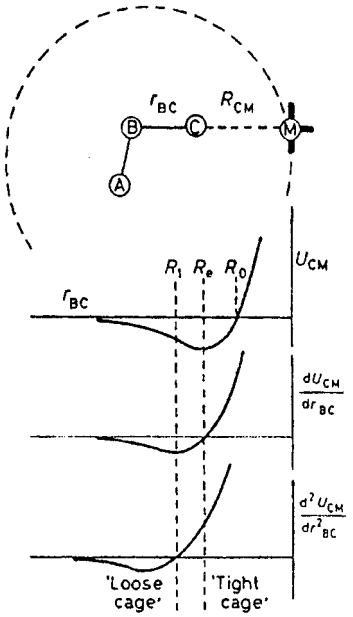

Figure 5. Dependence of interaction potential functions U, U', and U'' on matrix cage size (from Pimentel and Charles[13]).

$$B_e = \frac{h}{8\pi^2 m_r c r_e^2} \quad \text{and} \quad \omega_e = \frac{1}{2\pi c}\sqrt{\frac{k}{m_r}} \qquad (2)$$

$$\Delta\nu = \nu_{\text{matrix}} - \nu_{\text{gas}} = \frac{1}{4\pi c r_e^2 \sqrt{m_r k}}\left[U'' - \frac{3A}{\omega_e}U'\right] \qquad (3)$$

In eq 3, ν_{matrix} is the vibrational frequency of the trapped molecule in the matrix; m_r and k are the reduced mass and the harmonic force constant corresponding to the vibrational mode of the trapped molecule.

It can be seen from eq 3 that the sign of $\Delta\nu$ (positive or negative) is determined by the bracketed potential energy term, which in turn was shown to depend on the degree of freedom experienced by the solute molecule in a matrix cage.[13] Considering a bent triatomic molecule ABC trapped in a matrix cage formed by atoms M which are rigidly positioned by the lattice (Figure 5), Pimentel and Charles evaluated the contribution to energy U resulting from the interaction between C and M, as the internal coordinate r_{BC} changed due to the stretching vibration of the bond between B and C. Movements and interactions of other atoms were ignored in their treatment.[13]

The nature of the functions U_{C-M} and its first $(\partial U_{C-M}/\partial r_{BC})$ and second $(\partial^2 U_{C-M}/\partial r_{BC}^2)$ derivatives are shown in Figure 5. It can be seen that if the distance R_{CM} is greater than R_1 the effect of the matrix is to contribute negative quantities to both U' and U''. Since the anharmonicity constant A is a negative number, the bracketed potential energy term in eq 3 is negative, and hence, $\Delta\nu$ is negative; i.e., the vibrational frequency is lower in the matrix cage than in the free gas. Pimentel and Charles referred to this type of positioning, $R_{CM} > R_1$ as corresponding to a "loose" cage.[13] On the contrary, when R_{CM} is less than R_e (the optimum distance), both U'' and U' are positive. As constant A is negative, the bracketed potential energy term, and hence, $\Delta\nu$ is positive; i.e., the vibrational frequency in the matrix cage is greater than that in the free gas. Pimentel and Charles referred to this type of positioning, $R_{CM} < R_e$, as corresponding to a "tight" cage. For intermediate positions of atom C, i.e., $R_e < R_{CM} < R_1$, Pimentel and Charles concluded that the sign of $\Delta\nu$

TABLE 1: Frequencies (cm^{-1}) and Frequency Shifts of the Symmetric C−H Stretching Bands of CH_4, and the C−H Region Fermi Resonance Doublet Bands and Symmetric C−C Stretching Bands of Ethane, in Different Hydrate Cages

guest molecule	vibrational mode	ν_{gas}	cage type	cage diameter[a] (Å)	ν_{guest}	$\Delta\nu$[b]
methane CH_4[c]	ν_1 C−H symmetric stretching	2917.6[d]	sI large ($5^{12}6^2$)	5.86	2904.8	−12.8
			sI small (5^{12})	5.02	2915	−2.6
			sII large ($5^{12}6^4$)	6.57	2903.7	−13.9
			sII small (5^{12})	5.0	2913.7	−3.9
			sH large ($5^{12}6^8$)	8.62	*e*	*e*
			sH medium ($4^35^66^3$)	5.32	2905	−12.6
			sH small (5^{12})	5.02	2912.8	−4.8
ethane C_2H_6	C−H region Fermi resonance doublet bands	2900.4[f]	sI large ($5^{12}6^2$)	5.86	2891.2[f]	−9.2
					2946.2[f]	−9.4
		2955.6[f]	sII large ($5^{12}6^4$)	6.57	2887.3[f]	−13.1
					2942.3[f]	−13.3
	C−C symmetric stretching	994.4[f]	sI large ($5^{12}6^2$)	5.86	1000.9[f]	+6.5
			sI small (5^{12})	5.02	∼1020[g]	∼+25.6
			sII large ($5^{12}6^4$)	6.57	992.9[f]	−1.5
			sII small (5^{12})	5.0	∼1020[h]	∼+25.6

[a] Represents the free space available in a cage; calculated as free cage diameter = 2(average cage radius − 1.4 Å,) where 1.4 Å is the van der Waals radius of water molecule; average radii for sI and sII hydrate cages from refs 2 and 3; for sH, average cage radii were taken from Sloan.[1] [b] Frequency shift $\Delta\nu = \nu_{guest} - \nu_{gas}$. [c] ν_{guest} values for CH_4 in sI, sII, and sH obtained from Sum et al.[6] [d] Frequency at 3.4 MPa taken from Sum et al.[6] [e] No occupation of this cavity was observed (see Sum et al[6]). [f] Subramanian et al.[11] [g] Estimated from Figure 4 in Morita et al.[15] [h] This work.

will be determined by the relative magnitudes of U'' and U', and no generalizations can be made. [13]

The loose cage−tight cage model has been used to explain the observed vibrational frequency shifts $\Delta\nu$ ($=\nu_{matrix} - \nu_{gas}$) for several polyatomic molecules (such as NH_3, CO_2, methane) upon being trapped in low-temperature matrixes of molecules such as neon, argon, krypton, xenon, etc.[13,27−30] Specifically, the model has been used to explain the negative shifts (negative $\Delta\nu$) characteristic of a loose cage that have been observed for high frequency, high force constant stretching vibrations compared to positive shifts (positive $\Delta\nu$) characteristic of a tight cage observed for low frequency, low force constant bending vibrational modes for a molecule trapped in a particular matrix cage. It has also been used to show qualitatively that $\Delta\nu$ for a given vibration in a given matrix becomes progressively more positive with size of the trapped molecule because of the vibrations occurring in a progressively tight cage environment with increase in molecule size.[13,27−30] It has also been used to explain trends in stretching frequencies of guests in cages of β-quinol clathrate.[31] This clathrate is similar in nature to clathrate hydrates, and it was first discovered in 1947.[32]

The following general trends in vibrational frequencies are predicted by the loose cage−tight cage model for guests trapped in clathrate hydrate cages:

(1) For stretching modes, an increase in cage size implies a looser cage environment for the trapped molecule and, therefore, a more negative $\Delta\nu$. Hence, the larger the cavity, the lower the frequency of the stretching vibration.

(2) Increase in size of a molecule occupying a cage will cause $\Delta\nu$ for a stretching vibration to become more positive. This is because increasing repulsive interactions between the guest and the cage with guest size cause the vibration to occur in a progressively tight cage environment.

(3) High frequency, high force constant stretching vibrations in the molecule will show negative shifts (negative $\Delta\nu$) whereas low frequency, low force constant bending vibrations will show positive shifts (positive $\Delta\nu$).

(4) An increase in pressure will cause $\Delta\nu$ for the guest stretching vibration to become more positive. This is because a sufficient increase in pressure will cause lattice compression leading to a decrease in cage size and an increase in repulsive interactions between the guest and the cage. The vibration will then occur in a tight cage environment.

(5) For low frequency, low force constant bending modes in trapped molecules, the model predicts that "the larger the cavity, the higher the bending frequency or more positive the $\Delta\nu$". This trend is opposite of that predicted for stretching modes. An explanation for this can be found in the original work of Pimentel and Charles.[13]

Application of Model to Raman Spectra of Guests

In this section, predictions from the qualitative loose cage−tight cage model are compared with general trends in frequencies observed in the Raman spectra of methane, ethane, propane, and isobutane trapped in hydrate cages.

Dependence of Frequency Shifts on Cage Size for Guests Occupying Multiple Cages. Table 1 lists the totally symmetric C−H stretching frequencies of methane trapped in the different cages of sI, sII, and sH hydrates and the frequency shifts, $\Delta\nu$, corresponding to methane in each cage. Here, $\Delta\nu = \nu_{guest} - \nu_{gas}$, i.e., frequency for methane acting as a guest in a particular cage minus the frequency for methane in the free gas phase. The band assignments for methane in different cages are adopted from Sum et al.[6] They are based on band intensity ratios, relative numbers of different cage types in the hydrate, and estimated occupancy of each cage type.[6] Also listed in Table 1 are frequencies and frequency shifts ($\Delta\nu$) observed for the C−H region Fermi resonance doublet bands and the symmetric C−C stretching bands of ethane trapped in cages of sI and sII hydrates. The ν_{guest} and $\Delta\nu$ values for the C−C stretching vibration of ethane in the small 5^{12} cages of sI and sII hydrates correspond to high-pressure measurements (∼70 MPa).

From Table 1, it is clear that there is a distinct trend in frequencies and frequency shift $\Delta\nu$ for the C−H stretching vibration of methane between the different cages. In sI and sII hydrates, the frequency is lower by about 10 cm^{-1} and the $\Delta\nu$ value is more negative for methane trapped in the large cages ($5^{12}6^2$ or $5^{12}6^4$) compared to that of methane in the small 5^{12} cages. Comparing the large cages of sI and sII, we see that the frequency for methane in the $5^{12}6^4$ cage of sII is lower by 1.1 cm^{-1} and the $\Delta\nu$ value is more negative for that cage as well. For sH hydrate, we see that the frequency in the medium $4^35^66^3$ cage is lower by 7.8 cm^{-1} compared to that of the small 5^{12} cage.

Similarly, for the C−C stretching vibration of ethane in sI and sII hydrates, the frequency is lower and the $\Delta\nu$ values are

TABLE 2: Symmetric C−C Stretching Frequencies (cm^{-1}) of Ethane, Propane, and Isobutane in the Gas Phase and as Guests in the $5^{12}6^4$ Cage of sII Hydrate

molecule	guest diameter (Å)[a]	ν_{guest}	ν_{gas}	$\Delta\nu$[b]
C_2H_6[c]	5.5	992.9	994.4	−1.5
C_3H_8[d]	6.28	878	870.7	+7.3
i-C_4H_{10}[e]	6.5	811.7	798.9	+12.8

[a] Sloan.[1] [b] Frequency shift $\Delta\nu = \nu_{guest} - \nu_{gas}$. [c] See Table 1. [d] Sum et al.[6] [e] This work.

significantly more negative in the larger cages ($5^{12}6^2$ and $5^{12}6^4$) compared to those in the smaller 5^{12} cage (Table 1). Comparing the large cages of sI and sII, we see that the C−C stretching frequency in the $5^{12}6^4$ cage of sII is lower by 8 cm^{-1} and the $\Delta\nu$ value is more negative for that cage as well. Also, the perturbed frequencies of the C−H region resonance doublet bands of ethane are lower by 4 cm^{-1} in the $5^{12}6^4$ cage compared to those in the $5^{12}6^2$ cage.

On the basis of all of these observations, the general qualitative trend in the stretching frequencies of methane and ethane with cage size can be stated as "the larger the cavity, the lower the stretching frequency and the more negative the $\Delta\nu$". This trend is same as that predicted by the loose cage−tight cage model for stretching vibrations.

Quantitatively, it should be noted that despite similar differences in free diameter between the 5^{12} and $5^{12}6^2$ versus the $5^{12}6^2$ and $5^{12}6^4$ cages (0.84 versus 0.71 Å), the difference in C−H stretching frequencies of CH_4 for the two cases is 10.2 versus 1.1 cm^{-1}. These largely uneven differences in frequencies for similar changes in cage size can be explained using U' and U'' profiles in Figure 5. Close to the cage wall, i.e., $R_{CM} \ll R_e$ (tight cage environment such as CH_4 in 5^{12}), U' and U'', and hence $\Delta\nu$, change sharply with distance from the cage wall. At large distances from the cage wall, i.e., $R_{CM} \gg R_1$ (loose cage environment such as CH_4 in $5^{12}6^2$ and $5^{12}6^4$), U' and U'' profiles are flat. Hence, change in $\Delta\nu$ for the same change in distance will be much smaller. The same reasoning also applies for uneven differences in C−C stretching frequencies of ethane between different cages of sI and sII hydrates (Table 1).

Dependence of Frequency Shifts on Guest Size. Ethane, propane, and isobutane are expected to occupy only the large $5^{12}6^4$ cages in sII hydrate at low pressures (∼1−2 MPa). Their molecular size increases from 5.5 Å for ethane to 6.28 Å for propane to 6.5 Å for isobutane.[1] These three molecules have only one symmetric C−C stretching vibrational mode due to the existence of only one type of C−C bond in each molecule. It is, hence, worthwhile to consider trends in the symmetric C−C stretching frequencies as a function of guest size when the three molecules occupy the $5^{12}6^4$ cavity of sII hydrate. These frequencies along with the frequency shifts, $\Delta\nu$, are listed in Table 2. The trend evident from Table 2 is that as the size of the guest molecule trapped in the $5^{12}6^4$ cage increases, the $\Delta\nu$ values for the symmetric C−C stretching frequency become progressively more positive. This observed trend is consistent with the trend predicted by the loose cage−tight cage model.

Dependence of Frequency Shifts on Guest Vibrational Mode. To study the effect of enclathration on different stretching modes within a guest molecule, consider the case of ethane. As the low-frequency C−C stretching vibration (∼1000 cm^{-1}) has a slightly lower force constant (∼$4.5 \cdot 10^5$ dynes/cm) compared to the force constant of ∼$4.79 \cdot 10^5$ dynes/cm for the high-frequency C−H stretching vibration (∼2900 cm^{-1}),[33] the loose cage−tight cage model would predict that $\Delta\nu$ would be more negative for the C−H region bands than for the C−C stretching bands. Frequency shifts, $\Delta\nu$, listed in Table 1 for C−H region and C−C stretching bands of ethane in the $5^{12}6^2$ and $5^{12}6^4$ cages are consistent with this model prediction.

Dependence of Frequency Shifts on Pressure. Nakano et al. have reported that frequency of the C−H stretching vibration of methane in the small 5^{12} cage of sI hydrate increases monotonically with pressure from about 2915 cm^{-1} at 20 MPa to about 2919 cm^{-1} at 500 MPa.[12] However, the frequency for methane in the large $5^{12}6^2$ cage remains almost constant at 2905 cm^{-1} over the same pressure range.[12] These observations for methane in the 5^{12} cage are consistent with the trend predicted by the loose cage−tight cage model for the case of increase in pressure. For methane in the $5^{12}6^2$ cage, the weak dependence on pressure may be due to methane experiencing a considerably

TABLE 3: Frequencies (cm^{-1}) and Frequency Shifts for Vibrations of Ethylene Oxide, Acetylene, Carbon Dioxide, and Sulfur Dioxide in Different Cages of sI and sII Hydrates

guest molecule	vibrational mode	ν_{gas}	cage type	ν_{guest}	$\Delta\nu$[a]
ethylene oxide C_2H_4O	ν_3 C−O stretching	1270.3[b]	sI large ($5^{12}6^2$)	1266[c]	−4.3
			sI small (5^{12})	1281[c]	+10.7
			sII small (5^{12})	1279[c]	+8.7
acetylene C_2H_2[d]	ν_3 C−H stretching	3288.7	sI large ($5^{12}6^2$)	3261	−27.7
			sI small (5^{12})	3280.1	−8.6
			sII small (5^{12})	3274.2	−14.5
deuterated acetylene C_2D_2[d]	ν_3 C−D stretching	2439.2	sI large ($5^{12}6^2$)	2419	−20.2
			sI small (5^{12})	2430.6	−8.6
			sII small (5^{12})	2427.1	−12.1
carbon dioxide CO_2[e]	ν_3 C−O asymmetric stretching	2349.3[f]	sI large ($5^{12}6^2$)	2335	−14.3
			sI small (5^{12})	2347	−2.3
			sII small (5^{12})	2345	−4.3
	ν_2 CO_2 bending	667.3[f]	sI large ($5^{12}6^2$)	660	−7.3
			sI small (5^{12})	655	−12.3
			sII small (5^{12})	655	−12.3
sulfur dioxide SO_2[g]	ν_1 S−O symmetric stretching	1151.2[h]	sI large ($5^{12}6^2$)	1146	−5.2
			sI small (5^{12})	1151	−0.2
	ν_3 S−O asymmetric stretching	1361[h]	sI large ($5^{12}6^2$)	1342	−19.0
			sI small (5^{12})	1347	−14.0
	ν_2 SO_2 bending	519[h]	sI large ($5^{12}6^2$)	517	−2.0
			sI small (5^{12})	521	+2.0

[a] Frequency shift $\Delta\nu = \nu_{guest} - \nu_{gas}$. [b] See Bates.[34] [c] See Richardson et al.[35] [d] All frequencies (ν_{gas} and ν_{guest}) for C_2H_2 and C_2D_2 obtained from Consani and Pimentel.[36] [e] ν_{guest} values for CO_2 obtained from Fleyfel and Devlin.[37,38] [f] From p 274 in Herzberg.[33] [g] All ν_{guest} values for SO_2 obtained from Fleyfel and Devlin.[39] [h] From p 285 in Herzberg.[33]

loose cage environment in that cage despite the slight shrinkage of the $5^{12}6^2$ cage over the pressure range of 20−500 MPa. The same arguments can be made to explain observed trends in C−C stretching frequencies of ethane in the $5^{12}6^2$ and 5^{12} cages of sI hydrate over the pressure range of 20−479 MPa.[15]

Application of Model to Infrared (IR) Spectra of Guests

In this section, predictions from the loose cage−tight cage model are compared with general trends in frequencies observed in IR spectra of various guests. Table 3 is a compilation of frequencies (and corresponding $\Delta\nu$ values) for different vibrational modes obtained from IR spectra of several guests (ethylene oxide, acetylene, CO_2, and SO_2) trapped in sI and sII hydrate cages. From Table 3, it is evident that the stretching vibrations of ethylene oxide, C_2H_2, C_2D_2, and CO_2 trapped in the $5^{12}6^2$ cage of sI exhibit lower frequencies and more negative $\Delta\nu$ compared to the frequencies and $\Delta\nu$ for these guests trapped in the 5^{12} cages of sI and sII hydrates. A similar conclusion can be drawn for the stretching vibrations of SO_2 upon comparing frequencies and the $\Delta\nu$ values for the $5^{12}6^2$ and 5^{12} cages of sI hydrate. These trends from IR spectra are similar to those discussed in the previous section for Raman spectra and are consistent with the trend predicted by the model.

However, the agreement between experimental observations and model predictions are not as sound when frequency trends for bending modes of CO_2 and SO_2 are considered. Table 3 shows that the frequency of the ν_2 bending mode of CO_2 in the $5^{12}6^2$ cage of sI is 5 cm^{-1} higher than that in the 5^{12} cages of sI and sII hydrates. While this observed trend for CO_2 agrees well with the general trend predicted by the loose cage−tight cage model for low-frequency bending modes, the observed trend for SO_2 is in disagreement with the predicted general trend. Table 3 shows that the frequency of the ν_2 bending mode of SO_2 in the $5^{12}6^2$ cage is 4 cm^{-1} lower than that in the 5^{12} cage of sI hydrate. On the basis of this partial agreement between the model and experimental data for CO_2 and SO_2, we tentatively conclude that the model, while generally applicable, cannot always explain trends in bending frequencies of guests.

Anomalous Trend in Guest Stretching Frequencies for 5^{12} Cages of sI and sII

The small cages in sI and sII hydrates are pentagonal dodecahedra (5^{12}). X-ray diffraction data for sI EO hydrate[2] and sII THF + H_2S hydrate[3] suggest that the average radius of the sI 5^{12} cage (3.908 Å) is slightly greater than the average radius of the sII 5^{12} cage (3.902 Å). The data also suggest that the sI 5^{12} cage is more spherical than the sII 5^{12} cage (3.3% versus 5.3% variation in size or sphericity).

Although it is somewhat dangerous to generalize the results of X-ray diffraction work on a particular system and assume it to be representative of an overall behavior of hydrate-forming systems, some anomalous trends resulting from such a generalization are worth discussing. If we generalize that the 5^{12} cage of sII is slightly smaller than the 5^{12} cage of sI, the loose cage−tight cage model would predict that the stretching frequencies of guests would be slightly higher in the 5^{12} cage of sII hydrate. However, scrutinizing the observed stretching frequencies of methane in Table 1, and EO, acetylene (C_2H_2 and C_2D_2), and CO_2 in Table 3, we find an opposite trend. The frequencies in the slightly smaller sII 5^{12} cage are actually lower than frequencies in the sI 5^{12} cage. A similar anomaly can also be observed when trends in NMR chemical shifts of ^{129}Xe trapped in the 5^{12} cages of sI and sII hydrates are considered. The observed chemical shift trend between these two cages is opposite of that predicted by the linear correlation reported by Ripmeester et al. for ^{129}Xe chemical shift versus free radius of the cage.[40] Thus, spectral signatures from three different techniques, Raman, IR, and NMR, show similar anomalous trends between the 5^{12} cages of sI and sII hydrates.

Some of the factors that could cause these anomalous trends are as follows: (1) A lower sphericity of the sII 5^{12} cage could complicate the nature of the host−guest interaction potential in the cage resulting in multiple potential minima.[41] This in turn may cause certain preferred orientations of guests in the cage, resulting in their stretching vibrations experiencing a looser cage environment compared to when they are trapped in the almost spherical 5^{12} cage of sI.

(2) Factors other than the size of the cage could be contributing to the observed anomalous trend. The loose cage−tight cage model is simplistic and qualitative in nature and focuses mainly on the effect of cage size on the frequency shift.

(3) Occupation of the $5^{12}6^4$ cage by the large guest (such as THF) may be causing lattice distortions and, hence, expansion of the sII 5^{12} cage. This may contribute to the sII 5^{12} cage actually being larger than the sI 5^{12} cage for the Raman, IR, and NMR examples referred to in this section.

In summary, it is not completely clear at this point why the stretching frequencies of guests in the sII 5^{12} cage are lower than frequencies for the sI 5^{12} cage. This could be considered an anomaly provided the generalization that the 5^{12} cage in sII hydrate is smaller than that in sI is valid for all hydrate-forming systems.

Conclusions

Raman results obtained for sII ethane + THF hydrate at a pressure of 70.7 MPa indicate that ethane occupies the small 5^{12} cage at this pressure. Morita et al. have reported a similar conclusion based on their high-pressure Raman studies of sI ethane hydrate.[15] Raman spectrum of a sII isobutane hydrate was obtained for the first time. The symmetric C−C stretching vibration of isobutane in the $5^{12}6^4$ cage was found to occur at 811.7 cm^{-1}, which is 12.8 cm^{-1} higher than the frequency in the free gas phase.

On the basis of Raman spectra for liquid *n*-butane and sII methane + *n*-butane hydrate, it was demonstrated that only the gauche (boat) form of *n*-butane participates in the sII hydrate lattice. This selective behavior was attributed to the lower energy trans (chair) form being too large to occupy the $5^{12}6^4$ cage.

A qualitative literature model, explaining the effect of a matrix cage on the vibrational frequency of a guest in the cage, was briefly discussed. This loose cage−tight cage model was used to predict trends in vibrational frequencies of guest molecules trapped in hydrate cages. The model predictions were compared with trends in frequencies and frequency shifts observed in Raman and IR spectra of numerous guests. Specifically, observed and predicted trends with cage size, guest size, guest vibrational mode, and pressure were compared. For varying cage sizes, the trend predicted by the model and confirmed by the Raman and IR data, was "the larger the cavity, the lower the frequency of the stretching vibration of the guest".

There was also good agreement between predicted and observed trends for stretching frequencies as a function of guest size, vibrational mode, and system pressure. For guest bending modes, there was partial agreement between predicted and observed trends. By making a generalization about relative sizes of 5^{12} cages, a possible anomaly was inferred upon comparing trends in stretching frequencies of guests between the 5^{12} cages

of sI and sII hydrates. More research is needed to establish the validity of the generalization and the existence of the anomaly.

Overall, the simple loose cage−tight cage model correlating frequency shifts in IR and Raman spectra of guests to cage size works well and provides a qualitative explanation for a number of simple guests trapped in different hydrate cages.

Acknowledgment. This work was supported by the National Science Foundation, Grant No. CTS − 9634899. We thank Dr. Robert C. Burruss, U. S. Geological Survey, for helpful discussions and Prof. Paul Devlin, Oklahoma State University, for recommending the work of Pimentel and Charles.[13] Dr. Vu Thieu, currently at Baker Petrolite, Houston, designed and fabricated the optical cell used for high-pressure measurements.

References and Notes

(1) Sloan, E. D. *Clathrate Hydrates of Natural Gases*; Marcel Dekker: New York, 1998.
(2) McMullan, R. K.; Jeffrey G. A. *J. Chem. Phys.* **1965**, *42*, 2725.
(3) Mak, T. C. W.; McMullan, R. K. *J. Chem. Phys.* **1965**, *42*, 2732.
(4) Udachin, K. A.; Ratcliffe, C. I.; Enright, G. D.; Ripmeester, J. A. *Supramol. Chem.* **1997**, *8*, 173.
(5) Uchida, T.; Takagi, A.; Kawabata, J.; Mae, S.; Hondoh, T. *Energy Covers. Mgmt.* **1995**, *36*, 547.
(6) Sum, A. K.; Burruss, R. C.; Sloan, E. D. *J. Phys. Chem.* **1997**, *101*, 7371.
(7) Pauer, F.; Kipfstuhl, J.; Kuhs, W. F. *J. Geophys. Res.* **1997**, *102*, 26519.
(8) Nakano, S.; Moritoki, M.; Ohgaki, K. *J. Chem. Eng. Data* **1998**, *43*, 807.
(9) Tulk, C. A.; Ripmeester, J. A.; Klug, D. D. *Proceedings of the 3rd International Conference on Gas Hydrates, Annals of the New York Academy of Sciences*, Salt Lake City, **2000**, *912*, 859.
(10) Subramanian, S.; Sloan, E. D. *Fluid Phase Equilib.* **1999**, *158*−*160*, 813.
(11) Subramanian, S.; Kini, R. A.; Dec, S. F.; Sloan, E. D. *Chem. Eng. Sci.* **2000**, *55*, 1981.
(12) Nakano, S.; Moritoki, M.; Ohgaki, K. *J. Chem. Eng. Data* **1999**, *44*, 254.
(13) Pimentel, G. C.; Charles, S. W. *Pure Appl. Chem.* **1963**, *7*, 111.
(14) Thieu, V.; Subramanian, S.; Colgate, S. O.; Sloan, E. D. *Proceedings of the 3rd International Conference on Gas Hydrates, Annals of the New York Academy of Sciences*; Salt Lake City, **2000**, *912*, 983.
(15) Morita, K.; Nakano, S.; Ohgaki, K. *Fluid Phase Equilib.* **2000**, *169*, 167.
(16) Jeffrey, G. A. In *Inclusion Compounds*; Atwood, J. L., Davies, J. E. D., MacNichol, D. D., Eds.; Academic Press: London, 1984; Vol. 1, p 135.
(17) Culberson, O. L.; McKetta, J. J. *Petroleum Trans.* **1951**, *192*, 223.
(18) Long, X. Master's Thesis, Colorado School of Mines, 1994.
(19) Evans, J. C.; Bernstein, H. J. *Can. J. Chem.* **1956**, *34*, 1037.
(20) Verma, A. L.; Murphy, W. F.; Bernstein, H. J. *J. Chem. Phys.* **1974**, *60*, 1540.
(21) Kint, S.; Scherer, J. R.; Snyder, R. G. *J. Chem. Phys.* **1980**, *73*, 2599.
(22) Durig, J. R.; Wang, A.; Beshir, W. *J. Raman. Spectrosc.* **1991**, *22*, 683.
(23) Murphy, W. F.; Fernandez-Sanchez, J. M.; Raghavachari, K. *J. Phys. Chem.* **1991**, *95*, 1124.
(24) Murphy, W. F. *J. Raman. Spectrosc.* **1992**, *23*, 413.
(25) Davidson, D. W.; Garg, S. K.; Gough, S. R.; Hawkins, R. E.; Ripmeester, J. A. *Can. J. Chem.* **1977**, *55*, 3641.
(26) Buckingham, A. D. *Proc. R. Soc.: London* **1958**, *A248*, 169.
(27) Barnes, A. J. In *Vibrational Spectroscopy of Trapped Species*; Hallam, H. E., Ed.; Wiley: London, 1973; Chapter 4.
(28) Murchison, C. B.; Overend, J. *Spectrochim. Acta* **1971**, *27*A, 1509.
(29) Allavena, M.; Rysnik, R.; White, D.; Calder, V.; Mann, D. E. *J. Chem. Phys.* **1969**, *50*, 3399.
(30) King, C. M.; Nixon, E. R. *J. Chem. Phys.* **1968**, *48*, 1685.
(31) Cleaver, K. D.; Davies, J. E. D.; Wood, W. J. *J. Mol. Struct.* **1975**, *25*, 222.
(32) Palin, D. E.; Powell, H. M. *J. Chem. Soc.* **1947**, 208.
(33) Herzberg, Z. *Infrared and Raman Spectra;* D. von Nostrand Company: New York, 1951; p 193.
(34) Bates, F. E. Ph.D. Thesis, University of Alberta, 1978.
(35) Richardson, H. H.; Wooldridge, P. J.; Devlin, J. P. *J. Chem. Phys.* **1985**, *85*, 4387.
(36) Consani, K.; Pimentel, G. C. *J. Phys. Chem.* **1987**, *91*, 289.
(37) Fleyfel, F.; Devlin, J. P. *J. Phys. Chem.* **1988**, *92*, 631.
(38) Fleyfel, F.; Devlin, J. P. *J. Phys. Chem.* **1991**, *95*, 3811.
(39) Fleyfel, F.; Richardson, H. H.; Devlin, J. P. *J. Phys. Chem.* **1990**, *94*, 7032.
(40) Ripmeester, J. A.; Ratcliffe, C. I.; Tse, J. S. *J. Chem. Soc., Faraday Trans.* **1988**, *I84*, 3731.
(41) Davidson, D. W. *Can. J. Chem.* **1971**, *49*, 1224.